Structure of boroaluminosilicate glasses: Impact of $[Al_2O_3]/[SiO_2]$ ratio on the structural role of sodium

Q. J. Zheng,[1,2] R. E. Youngman,[2,*] C. L. Hogue,[2] J. C. Mauro,[2] M. Potuzak,[2] M. M. Smedskjaer,[2] and Y. Z. Yue[1,3]

[1]*Section of Chemistry, Aalborg University, DK-9000 Aalborg, Denmark*

[2]*Science & Technology Division, Corning Incorporated, Corning, New York 14831, USA*

[3]*Shandong Key Laboratory of Glass and Ceramics, Shandong Polytechnic University, 250353 Jinan, China*

(Received 28 March 2012; published 22 August 2012)

In order to explore the structural roles of sodium in boroaluminosilicate glasses, we have designed ten Na_2O-B_2O_3-Al_2O_3-SiO_2 glasses with varied $[Al_2O_3]/[SiO_2]$ ratio to access different regimes of sodium behavior. Multinuclear nuclear magnetic resonance (NMR) experiments on ^{11}B, ^{27}Al, ^{29}Si, and ^{23}Na were performed to determine the complicated network former speciation and modifier environments as a function of glass composition. The different roles of sodium in relation with the network-forming cations (Si, B, and Al) have been clarified and quantified. When $[Na_2O] < [Al_2O_3]$, all available sodium is used to charge compensate fourfold coordinated aluminum (Al^{IV}), and deficiency in sodium concentration leads to fivefold coordinated aluminum (Al^{V}) groups. When $[Na_2O] > [Al_2O_3]$, sodium first charge compensates Al^{IV}, and thus all aluminum is fourfold coordinated and unaffected by other compositional changes. Hence, the preference in the formation of Al^{IV} over that of fourfold coordinated boron (B^{IV}) is confirmed. Excess sodium can be used to convert threefold coordinated boron (B^{III}) to B^{IV} or to create nonbridging oxygen (NBO) on Si and B, with a thermodynamic competition among these mechanisms. The NBOs on Si are quantified using ^{29}Si wide-line and magic angle spinning NMR. The fraction of silicon atoms associated with NBOs is calculated using a random model and compared with the NMR results. Finally, we have found that our previously proposed two-state statistical mechanical model of boron speciation accurately predicts the fraction of tetrahedrally coordinated boron atoms (N_4) in these mixed network former glasses.

DOI: 10.1103/PhysRevB.86.054203 PACS number(s): 61.43.Fs, 82.56.Hg, 81.05.Kf

I. INTRODUCTION

The macroscopic properties of a glass are the direct result of its microscopic structure,[1–7] as determined to a large extent by its chemical composition. In order to develop an enhanced understanding of structure-property relationships in glasses, it is thus critical to quantify the composition dependence of structural motifs within the glass network. This task is made especially difficult due to the lack of long-range structural order in glasses, which prevents the application of conventional structural characterization techniques such as x-ray diffraction. Alternative techniques, such as nuclear magnetic resonance (NMR) spectroscopy, have been particularly useful for elucidating many important aspects of both the short- and intermediate-range structural order in glass, especially in compositionally simple systems.[8,9] However, commercial glasses of industrial interest are typically multicomponent, and many unsolved structural puzzles still remain. Boroaluminosilicate glasses constitute a particularly important class of industrial material,[10–12] having found widespread applications in fields such as liquid crystal display substrates, optical components, fiberglass, radioactive waste containment, and photochromic glass. Understanding structure-property correlations in these glasses is especially challenging due to the mixed network former effect, which makes the structural speciation significantly more complicated.[13–15] In this paper, we present a detailed NMR study of network structure in this commercially important boroaluminosilicate glass system and evaluate several models for predicting network former speciation.

The role of network modifier cations in borate-containing glasses has been systematically investigated in prior studies.[16–20] In binary alkali borate glasses, the addition of a network modifier (such as Na_2O) to pure B_2O_3 initially converts threefold coordinated boron (B^{III}) to a fourfold coordination state (B^{IV}), with the network modifier cations acting as charge compensators for B^{IV}. The fraction of tetrahedral to total boron (N_4) reaches a maximum value with further modifier addition, when formation of nonbridging oxygen (NBO) becomes prevalent. In sodium borosilicate glasses, the empirical Dell–Bray model[21–23] is frequently invoked to predict N_4 and NBO concentrations as a function of glass composition. In this study, we consider quaternary sodium boroaluminosilicate glasses, the structure of which is more complicated due to the ability of sodium ions to interact not only with boron and silicon, but also with aluminum. Yamashita *et al.*[24,25] found that, in alkali boroaluminosilicate systems, when the three network formers coexist, the alkali oxides react preferably with Al_2O_3, and the value of N_4 can be estimated as $r/(1-r)$, where $r = ([Na_2O] - (Al_2O_3])/([Na_2O] - [Al_2O_3] + [B_2O_3])$. Stebbins *et al.*[13–15,26,27] have conducted a significant amount of work on understanding the structure of boroaluminosilicate glasses, e.g., they developed a modified Dell–Bray model[21–23] to account for their experimentally determined N_4 values. Smedskjaer *et al.* have recently introduced a new statistical mechanical model of boron speciation for accurate prediction of both the composition and thermal history dependence of boron speciation in borosilicate glasses.[28] In this model, the addition of network modifiers leads to a thermodynamic competition between the formation of NBO and the conversion of boron from trigonal to tetrahedral configuration. The model offers improved prediction of boron speciation and provides a natural

explanation for the observed thermal history dependence of N_4.

Nevertheless, cation speciation in complex oxide glasses is not yet fully understood, especially with the inherent competition between network modifiers and at least three different glass-forming oxide constituents. A new model that can better predict N_4 needs to be developed for such materials, since boron speciation is a very important parameter controlling several glass properties.[7] The network former speciation and modifier environments are determined by different structural roles (e.g., charge compensation) of sodium in sodium boroaluminosilicate glasses. In order to gain more knowledge of this system, we have studied ten Na_2O-B_2O_3-Al_2O_3-SiO_2 glasses with systematic variation of the $[Al_2O_3]/[SiO_2]$ ratio to access different regimes of sodium behavior: (1) Na^+ to stabilize aluminum in a tetrahedral configuration, (2) Na^+ to convert boron from trigonal to tetrahedral coordination, and (3) Na^+ to form NBO on silicon or boron. We obtain thorough structure details, e.g. network speciation and modifier cation environment, from a multinuclear NMR study of all cations (^{11}B, ^{27}Al, ^{29}Si, and ^{23}Na) using both magic angle spinning (MAS) and triple quantum (3Q) MAS NMR spectroscopy. Based on the resulting structural information, the different roles of Na_2O as a modifier are discussed in detail. We also extend the two-state statistical mechanical model of boron speciation, originally developed for borosilicate glasses, to these sodium boroaluminosilicate glasses, showing excellent agreement between predicted and measured N_4 values. This comprehensive study of alkali boroaluminosilicate glasses provides additional insight into glass structure and will serve as an important contribution to understanding and developing more complex multicomponent oxide glasses.

II. EXPERIMENTAL

A. Sample preparation

The batched compositions of the glasses were $x$$Al_2O_3-5B_2O_3$-(80-$x$)$SiO_2-15Na_2O$ with x = 0, 1, 2.5, 5, 7.5, 10, 12.5, 15, 17.5, and 20 (mol%). The analyzed compositions were slightly different from the batched compositions, but we retain the original naming convention based on $x$$Al_2O_3$, as listed in Table I. Figure 1 shows the ternary B_2O_3-Al_2O_3-SiO_2 composition diagram (mol%) plus 15% Na_2O and fining agent. We keep the Na_2O content constant in order to calculate the concentrations of B_2O_3, Al_2O_3, and SiO_2 in this diagram. All glasses were prepared by conventional melt quenching methods. The batch materials used in glass melting were SiO_2, Al_2O_3, H_3BO_3, and Na_2CO_3. Here, 0.1 mol% As_2O_3 or SnO_2 was added as a fining agent. The batch materials were mixed and then melted in a covered silica crucible at different homogenization temperatures T_h (see Table I) for 6 h in air. The melts were quenched in water, and the resulting glass shards were crushed and remelted for another 6 h at their respective melting temperatures to ensure chemical homogeneity. Finally, the melts were poured onto a stainless steel plate to obtain glasses. The glasses were annealed for 2 h at different temperatures (between 450 and 560 °C) depending on chemical composition. The chemical compositions of the

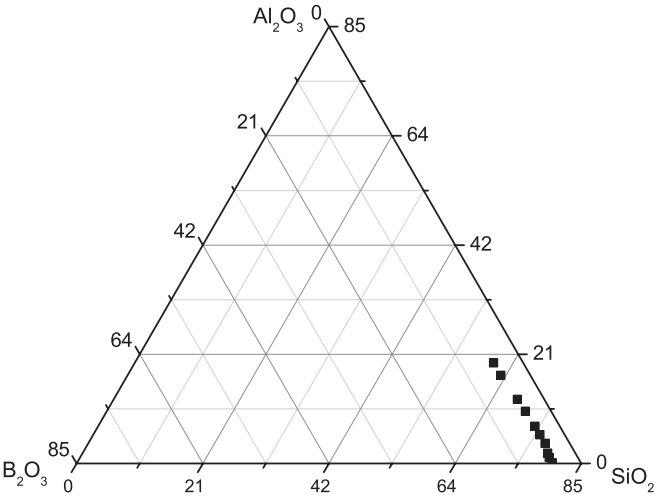

FIG. 1. The designed glass compositions indicated in the B_2O_3-Al_2O_3-SiO_2 diagram (85 mol% in total). 15 mol% Na_2O is not included in the composition diagram.

TABLE I. Analyzed chemical compositions, homogenization temperature (T_h), glass transition temperature (T_g), and fraction of tetrahedral to total boron (N_4) of the boroaluminosilicate glasses.

	Compositions (mol%)							
Glass ID	SiO_2	Al_2O_3	B_2O_3	Na_2O	Fining agent	T_h(°C)	T_g[a](K)	N_4(at%)
Al0	80.08	0.16	4.84	14.77	0.15	1450	809	94.9
Al1	79.38	1.16	4.85	14.60	0.14	1450	814	93.2
Al2.5	78.80	2.00	4.70	14.40	0.08	1450	822	94.6
Al5	78.10	4.00	4.20	13.60	0.07	1500	837	91.6
Al7.5	76.90	5.70	4.30	13.00	0.06	1550	851	83.1
Al10	75.90	7.50	4.30	12.30	0.07	1600	871	74.4
Al12.5	72.00	10.40	4.40	13.10	0.07	1650	887	43.6
Al15	69.20	12.70	4.60	13.50	0.07	1650	899	19.9
Al17.5	62.97	17.18	4.99	14.73	0.13	1650	956	1.0
Al20	60.52	19.61	5.00	14.73	0.14	1650	966	0.8

[a]T_g was obtained by fitting viscosity data with MYEGA equation (Ref. 29) and determined as the temperature at which equilibrium viscosity is 10^{12} Pa s.[7] The uncertainty of T_g is approximately ± 5 K. Al0, Al1, Al17.5 and Al20 used SnO_2 as fining agent while the rest of these glasses used As_2O_3 as a fining agent.

glasses, as reported in Table I, were determined by traditional wet chemistry methods.

B. Nuclear magnetic resonance

The annealed glass samples were ground for NMR experiments using an agate mortar and pestle. All NMR experiments were performed on commercial NMR spectrometers (Chemagnetics Infinity, Agilent VNMRS). ^{27}Al NMR experiments were conducted using an 11.7 T wide-bore superconducting magnet (Oxford). The resonance frequency of ^{27}Al at this magnetic field was 130.22 MHz. The ground glass samples were packed into 2.5 mm zirconia rotors having low Al background. Nuclear magnetic resonance spectra were collected using a 2.5 mm double-resonance MAS NMR probe, with spinning speeds of 22 kHz. ^{27}Al MAS NMR spectra were acquired with short radio-frequency pulses of 0.6 μs ($\pi/12$ tip angle) and signal averaging of nominally 1000 scans using a recycle delay of 1 s. ^{27}Al 3QMAS NMR spectra were collected using a hypercomplex 3QMAS pulse sequence with a Z filter.[30] The solid $\pi/2$ and $3\pi/2$ pulse widths were optimized to 0.7 and 2.0 μs, respectively. A lower power $\pi/2$ pulse width of 15.0 μs was used as the soft reading pulse of the Z filter. ^{27}Al 3QMAS NMR data were typically collected using 512 to 1024 acquisitions at each of 48 to 60 t_1 points, with a recycle delay of 0.2 to 0.5 s. The ^{27}Al NMR data were processed with commercial software using minimal line broadening (zero whenever possible) and referenced to aqueous aluminum nitrate at 0.0 ppm.

^{11}B NMR experiments were also conducted using an 11.7 T wide-bore superconducting magnet (Oxford). The resonance frequency of ^{11}B at this magnetic field was 160.34 MHz. The ground glass samples were packed into 3.2 mm zirconia rotors, and the NMR spectra were collected using a 3.2 mm double-resonance MAS NMR probe, with spinning speeds of 20 kHz. Short radio-frequency pulses ($\pi/12$ tip angle) were used for quantitative excitation of MAS NMR spectra. ^{11}B 3QMAS NMR spectra were collected using the same pulse sequence as for ^{27}Al, with solid $\pi/2$ and $3\pi/2$ pulse widths of 1.1 and 2.5 μs, respectively. The soft reading pulse of the Z filter was calibrated to 20.0 μs. ^{11}B 3QMAS NMR data were typically collected using 1024 acquisitions at each of 160 to 256 t_1 points, with a recycle delay of 1 s. The ^{11}B NMR data were processed with commercial software, without apodization and were referenced to aqueous boric acid at 19.6 ppm (relative to the standard BF_3-Et_2O).

^{23}Na NMR experiments were also conducted at 11.7 T (132.19 MHz resonance frequency). The ground glass samples were packed into 3.2 mm zirconia rotors, and the NMR spectra were collected using a 3.2 mm double-resonance MAS NMR probe, with spinning speeds of 20 kHz. Short radio-frequency pulses ($\pi/12$ tip angle) were used for excitation of MAS NMR spectra. 3QMAS NMR of ^{23}Na was also conducted using the Z-filtered hypercomplex pulse sequence described above, with solid $\pi/2$ and $3\pi/2$ pulse widths of 1.2 and 2.8 μs, respectively. The Z filter reading pulse was set to 15.0 μs. ^{23}Na 3QMAS NMR data were collected with signal averaging of 1000 scans at each of 36 t_1 points, all with a recycle delay of 1 s. The ^{23}Na NMR data were processed with minimal line broadening (zero if possible) and referenced to aqueous NaCl at 0.0 ppm.

^{29}Si wide-line (static) and MAS NMR experiments were conducted using a 4.7 T superconducting magnet (39.7 MHz resonance frequency). All experiments made use of a 7.5 mm MAS NMR probe, although samples were held static for the wide-line NMR experiments. The samples were packed into ZrO_2 rotors and MAS NMR data were collected at a spinning rate of 4 KHz, using a short radio-frequency pulse ($\pi/6$) with a long recycle delay (180 s). Signal averaging of $\sim$1000 acquisitions was necessary to obtain ^{29}Si MAS spectra of sufficient quality. All NMR spectra were processed with modest line broadening (50 Hz) and were externally referenced to TMS (0 ppm).

III. RESULTS

A. ^{27}Al NMR

The ^{27}Al MAS NMR spectra of the ten mixed network-former glasses are shown in Fig. 2. These data confirm the strong association between Na^+ and tetrahedral aluminum groups (Al^{IV}). When $[Na_2O] \geqslant [Al_2O_3]$, the spectra all consist of a narrow peak centered at around $+50$ ppm, consistent with Al^{IV}.[31] The spectra for glasses with $[Na_2O] \geqslant [Al_2O_3]$ are thus all very similar to one another, both in position and shape of the ^{27}Al resonance, which indicates that there is no significant difference in the Al^{IV} environment as a function of glass composition. For the two peraluminous glasses (Al17.5 and Al20), the ^{27}Al MAS NMR spectra are significantly and asymmetrically broader, mainly on the more shielded side (lower shift), which indicates the presence of higher Al coordination.[31] As shown by the overlay in Fig. 3, these two spectra contain different Al species, which can either be

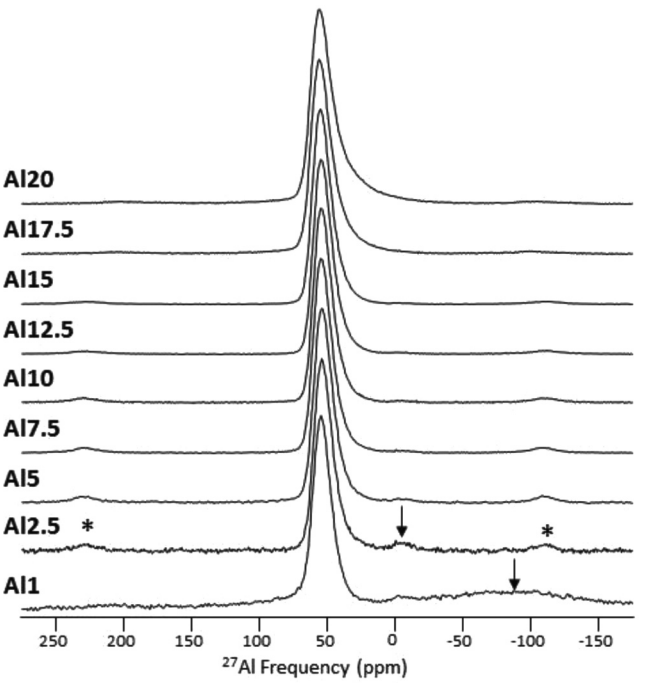

FIG. 2. ^{27}Al MAS NMR spectra of the boroaluminosilicate glasses as described and labeled in Table I. The asterisks mark spinning sidebands, and arrows denote background signal from rotor components, which is only seen at the lowest $[Al_2O_3]$.

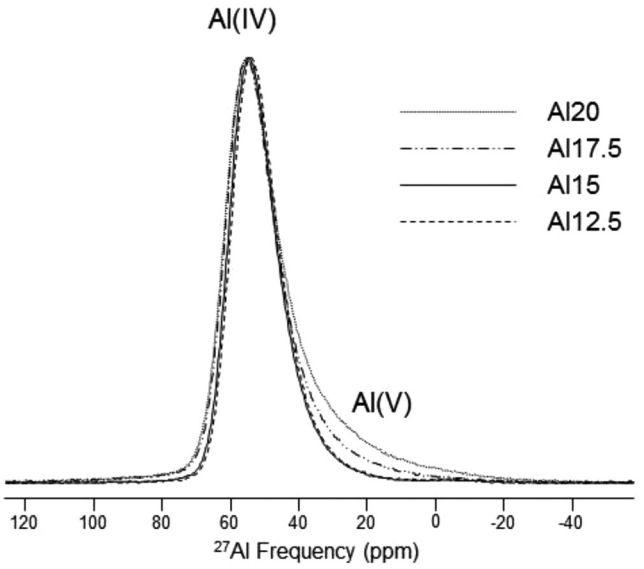

FIG. 3. Overlay of the ^{27}Al MAS NMR spectra from the four glasses containing the highest $[Al_2O_3]$.

spectrally subtracted from one another, or more precisely, simulated to reproduce MAS NMR line shapes for both the Al^{IV} and a second resonance around $+30$ ppm. The latter is consistent with Al^{V} groups.[31]

Two-dimensional ^{27}Al 3QMAS NMR spectra of representative glasses containing low (Al2.5) and high (Al17.5) $[Al_2O_3]$ are shown in Fig. 4. 3QMAS NMR spectroscopy provides higher resolution for quadrupolar nuclei such as ^{27}Al, enabling better resolution of different coordination environments in the isotropic dimension. In the case of the Al2.5 glass, the ^{27}Al 3QMAS NMR spectrum contains only a single set of contours, consistent with the MAS NMR spectra in Figs. 2 and 3, and the presence of only Al^{IV} polyhedra. In contrast, the ^{27}Al 3QMAS NMR spectrum of the Al17.5 glass contains a similar set of contours from a large quantity of Al^{IV} groups, as well as a barely detectable second signal attributed to a small fraction of Al^{V} groups. This is also consistent with the ^{27}Al MAS NMR data where, for $[Al_2O_3] > [Na_2O]$, the glasses appear to contain at least two different Al resonances.

B. ^{11}B NMR

^{11}B MAS NMR spectra of the ten glasses are shown in Fig. 5. These spectra are characterized by a broad peak centered at $+10$ ppm, corresponding to B^{III} sites, and a relatively narrow peak centered around -2 ppm, corresponding to B^{IV} sites. The relative peak intensities vary with composition, as evident in Fig. 5, which reflects changes in the relative proportions of B^{III} and B^{IV}. When $[Al_2O_3] \leqslant [Na_2O]$ (i.e., Al0 through Al15), these MAS NMR spectra show the presence of both B^{III} and B^{IV}. When $[Al_2O_3] > [Na_2O]$, most of the boron atoms exist in trigonal groups, with little evidence for the B^{IV} resonance. The fraction of B^{IV} (N_4) was determined by fitting the ^{11}B MAS NMR spectra in Fig. 5 and is reported in Table I for the entire series of glasses. We find that N_4 decreases with increasing $[Al_2O_3]$.

In addition to the boron coordination changes, the ^{11}B MAS NMR spectra in Fig. 5 reveal changes in the B^{III} NMR line

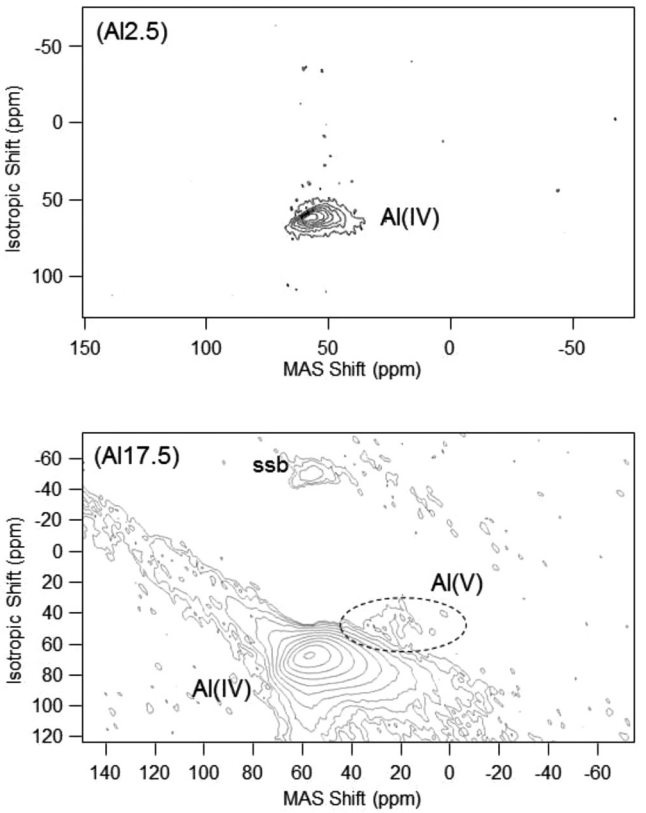

FIG. 4. ^{27}Al 3QMAS NMR spectra of two representative glasses containing low (Al2.5) and high (Al17.5) $[Al_2O_3]$. Contours from different Al coordination environments, as well as spinning sidebands (ssb), are denoted.

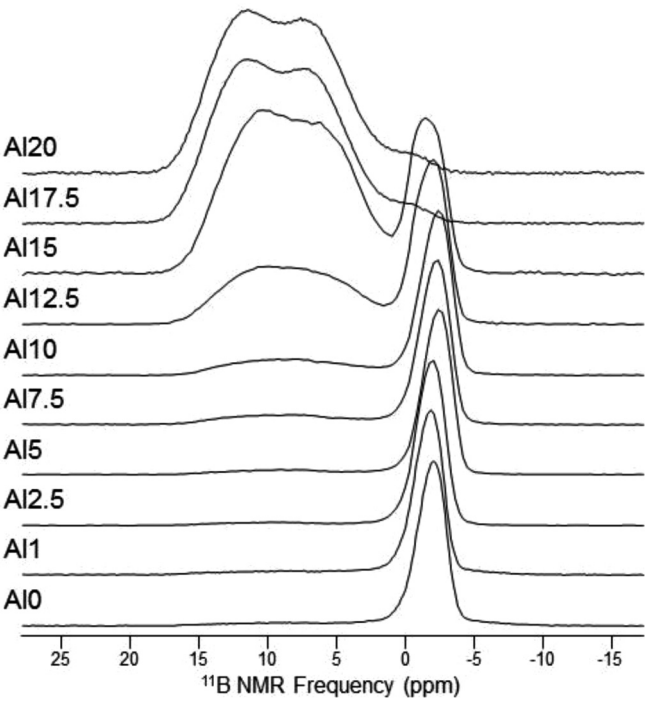

FIG. 5. ^{11}B MAS NMR spectra of the boroaluminosilicate glasses as described and labeled in Table I.

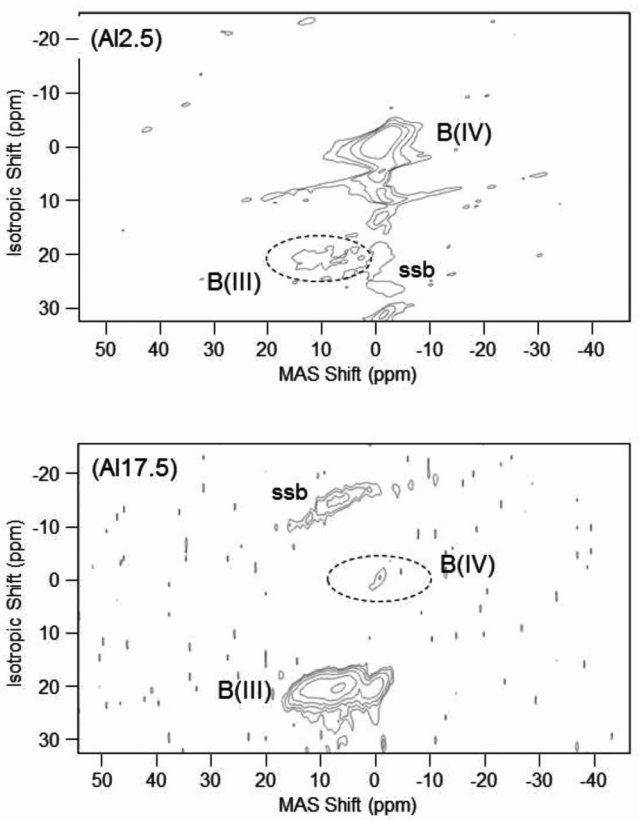

FIG. 6. ^{11}B 3QMAS NMR spectra of two representative glasses containing low (Al2.5) and high (Al17.5) [Al_2O_3]. The two different boron resonances are denoted, along with any spinning sidebands (ssb).

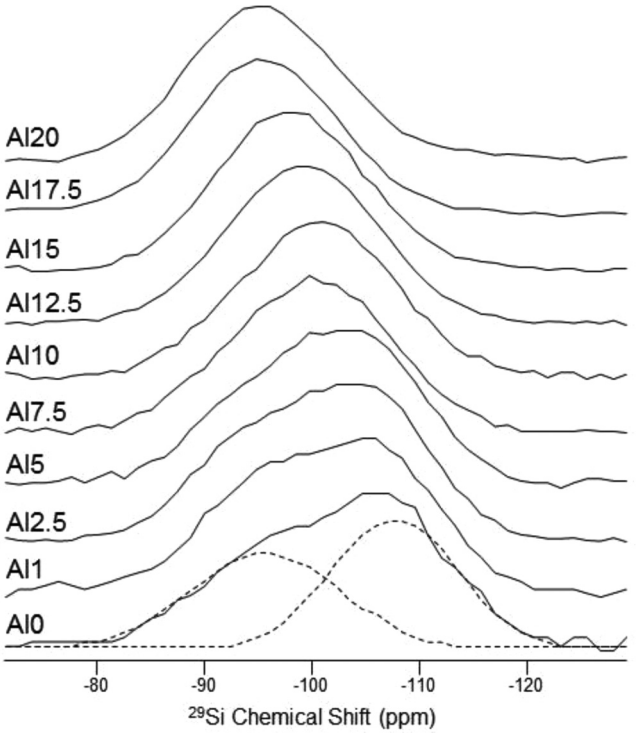

FIG. 7. ^{29}Si MAS NMR spectra of the boroaluminosilicate glasses. The spectra are labeled as in Table I. The spectrum of Al0 includes a Gaussian deconvolution into two distinct resonances (dashed lines).

shape, indicating some impact of glass composition on the short-range structure around trigonal boron. The frequency and line width of the B^{IV} resonances also change with composition, but such changes are not necessarily systematic with glass composition. This could indicate multiple types of B^{IV} sites or changes in local environment due to differing next nearest neighbors or intermediate-range order.

^{11}B 3QMAS NMR spectra of representative glasses containing low (Al2.5) and high (Al17.5) [Al_2O_3] are shown in Fig. 6. These spectra confirm the presence of multiple boron sites (i.e., both B^{III} and B^{IV} sites). More importantly, the data for the high [Al_2O_3] glass contain a small quantity of B^{IV} units, which is not immediately obvious in the ^{11}B MAS NMR spectra in Fig. 5 due to overlapping MAS NMR line shapes.

C. ^{29}Si NMR

^{29}Si MAS NMR spectra of the ten boroaluminosilicate glasses are shown in Fig. 7. There are clear changes in these spectra as a function of glass composition, with a systematic deshielding (to higher chemical shift) of the signal as [Al_2O_3] increases. In addition to this shift, the spectra, particularly at lower values of [Al_2O_3], also appear to be comprised of at least two separate resonances, which can be fit to a sum of Gaussian line shapes, as shown for the Al0 MAS NMR spectrum.

Further details of the silicon speciation, especially with respect to numbers of bridging and nonbridging oxygen, can be obtained by analysis of ^{29}Si wide-line (static) NMR spectral line shapes. This is because symmetry around the silicon atom controls the static NMR powder patterns. Figure 8 shows a stack plot of the ^{29}Si wide-line NMR spectra for the ten glasses, indicating that the overall line shape does change with composition. The spectra for low [Al_2O_3] glasses are highly asymmetric, with a pronounced feature on the deshielded side of the main peak near -100 ppm. As [Al_2O_3] increases, the ^{29}Si wide-line spectrum becomes broader and less asymmetric, reflecting changes in the Si speciation of these glasses, consistent with the ^{29}Si MAS NMR data.

D. ^{23}Na NMR

Figure 9(a) shows the ^{23}Na MAS NMR spectra of the ten glasses. These MAS NMR data show what appears to be a single, asymmetric resonance for all of the glasses. However, the line shape is sensitive to glass composition, with a significant narrowing of the resonance with increasing [Al_2O_3] [Fig. 9(b)]. The ^{23}Na MAS NMR spectra of the high [Al_2O_3] glasses also appear to be considerably less asymmetric than spectra for glasses containing low [Al_2O_3].

Two-dimensional ^{23}Na 3QMAS NMR spectra of representative glasses containing low (Al2.5) and high (Al17.5) [Al_2O_3] are shown in Fig. 10. Both sets of contour plots contain a single sodium resonance, which was also found for the entire series of compositions (data not shown). These data were further analyzed to determine average values of isotropic chemical shift (δ_{CS}) and quadrupolar coupling product (P_Q) for ^{23}Na in all glass samples (Table II).

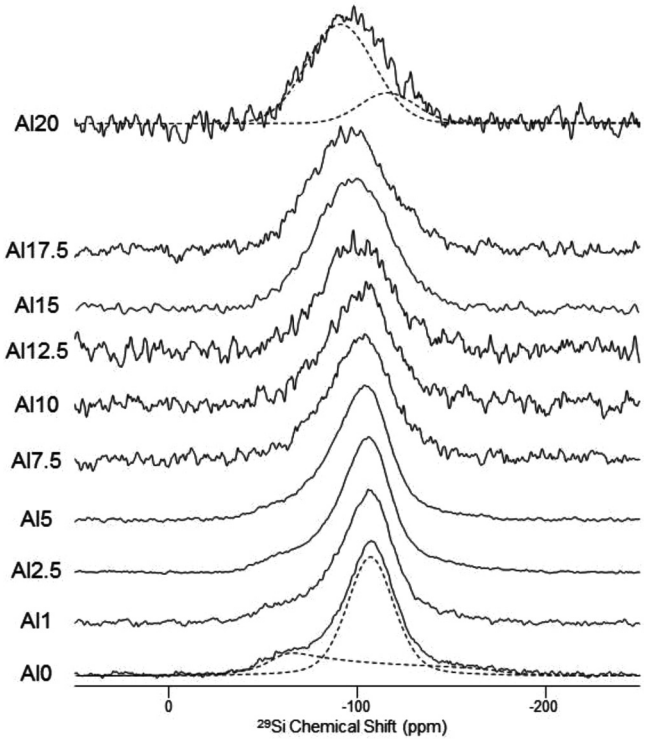

FIG. 8. Wideline ^{29}Si NMR spectra of the boroaluminosilicate glasses. The spectra are labeled using the naming convention in Table I. Dashed lines denote line shape simulations as described in the text.

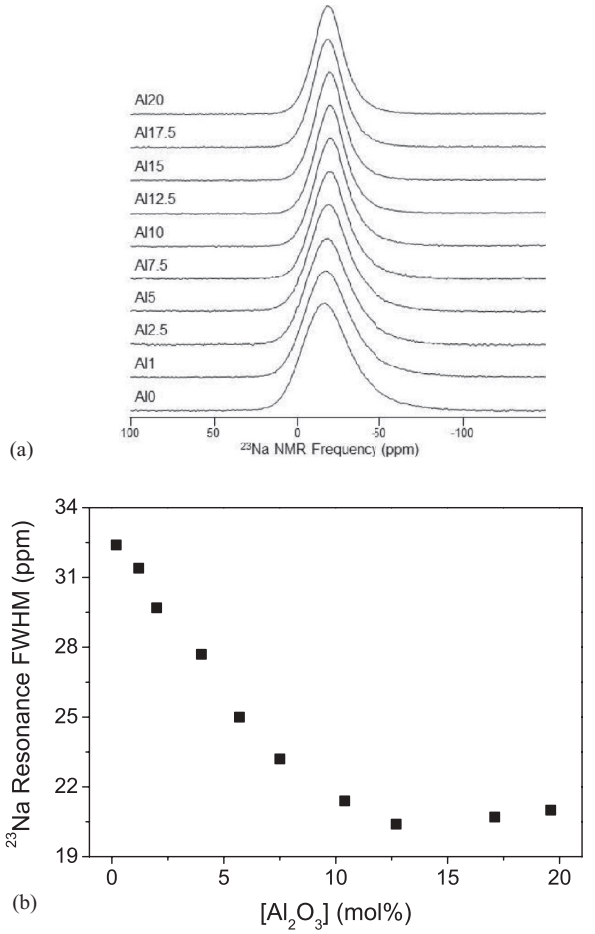

FIG. 9. (a) ^{23}Na MAS NMR spectra of the boroaluminosilicate glasses. The spectra are labeled using the naming convention in Table I. (b) Full width at half maximum (FWHM) of the ^{23}Na resonance as a function of $[Al_2O_3]$.

IV. DISCUSSION

A. Aluminum speciation

The ^{27}Al MAS and 3QMAS NMR results reported here clearly indicate that the aluminum-to-sodium ratio controls Al speciation. For the peralkaline compositions, there is sufficient Na^+ to stabilize all aluminum in fourfold coordination, and thus only a single Al resonance is detected in the ^{27}Al NMR spectra. These Al^{IV} environments are mostly unchanged when altering the amount of Al_2O_3 in the glasses. There are thus only minor changes in NMR parameters, particularly for P_Q, as shown in Table II, which are likely within the error of measurement or potentially a consequence of structural disorder. There is no obvious systematic change in either δ_{CS} or P_Q as a function of composition, which would be consistent with cation ordering around the Al^{IV} tetrahedra as the glass-former ratios are changed (e.g., decreasing Si next nearest neighbor (NNN) with increasing $[Al_2O_3]$).

For the peraluminous compositions, a small fraction of Al^V is detected in both the ^{27}Al MAS and 3QMAS NMR data. This asymmetric broadening of the MAS NMR spectra in Figs. 2 and 3 occurs in the region around $[Na_2O] = [Al_2O_3]$, where the onset of Al^V formation would be expected.[31] Furthermore, a distinct second resonance, which can be assigned to Al^V groups, is detected in the 3QMAS NMR spectra of the two peraluminous glasses (Fig. 4). Based on analysis of the ^{27}Al MAS NMR line shapes for the Al17.5 and Al20 glasses (Fig. 3), we are able to quantify the relative proportions of Al^{IV} and Al^V. We roughly estimate ($\pm$3%) that there exists 10% of the total Al as Al^V in the Al20 glass and 4% of the total Al as Al^V in the Al17.5 glass, both consistent with peraluminous compositions requiring Al^V polyhedra for proper charge balancing.[32] As indicated by the weak peak intensities, the population of Al^V is less obvious in the 3QMAS NMR spectra, similar to other reported data for aluminosilicate glasses.[33] By significantly expanding the vertical scales of these data (Fig. 4) and looking in the noise, we confirm the presence of Al^V and are therefore confident that the changing ^{27}Al MAS NMR line shapes are a result of increasing Al^V concentration when $[Al_2O_3] > [Na_2O]$.

This fivefold coordination environment around Al is expected for such compositions, where the amount of charge-balancing modifier cations (Na^+) is insufficient to stabilize all Al in fourfold coordination. As a consequence, some higher coordination Al species are formed and believed to provide an additional source of charge compensation in these networks.[31,32] Binary SiO_2-Al_2O_3 glasses with $[Al_2O_3] > 1$ wt% contain a mixture of Al^{IV}, Al^V, and Al^{VI} species.[31,32] The relative proportions of these species depend strongly on composition, and the high-coordinated Al species serve as charge compensators of tetrahedral Al^{IV} species. However, the addition of alkalis to these binary glasses results in the rapid disappearance of Al^V and Al^{VI} and stabilization of

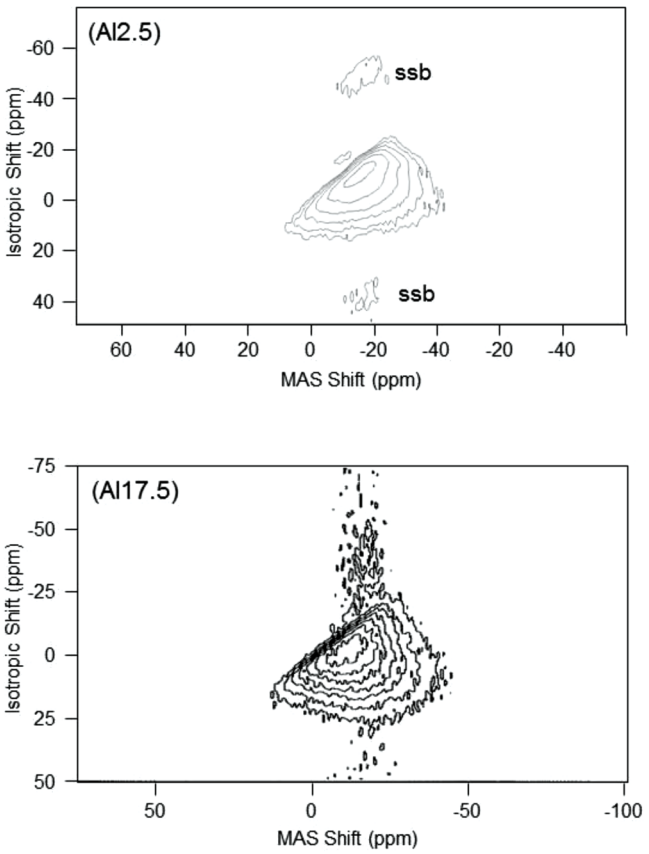

FIG. 10. ^{23}Na 3QMAS NMR spectra of two representative glasses containing low (Al2.5) and high (Al17.5) [Al_2O_3].

Al^{IV}.[32] A careful analysis of the high [Al_2O_3] glasses in the present study (Al17.5 and Al20) using both ^{27}Al MAS and 3QMAS NMR spectroscopy shows that only Al^{IV} and Al^{V} polyhedra are present, indicating that the amount of excess Al_2O_3 (i.e., [Al_2O_3] − [Na_2O]) is small and does not lead to the formation of Al^{VI} groups. These results confirm that we can confidently use the difference ([Na_2O] − [Al_2O_3]) to calculate an effective modifier concentration in a pseudoternary sodium borosilicate glass. The Al speciation is completely controlled by the sodium-to-aluminum ratio, viz., for [Al_2O_3] < [Na_2O], we can simply subtract [Al_2O_3] from [Na_2O] to get the amount of modifier left to act in other roles, including stabilization of B^{IV} and creation of NBOs, as discussed later. Similarly, the two glasses for which [Al_2O_3] > [Na_2O] appear to consume all Na^+ in charge-balancing Al tetrahedra, with a small fraction of Al^{V} to account for the insufficient amount of sodium, and more importantly, no modifier available for acting in other charge-balancing roles.

B. Boron speciation

Evidence for the above-mentioned behavior is also found in the ^{11}B MAS NMR spectra (Fig. 5), which show a large variation of boron speciation as a function of composition. At low [Al_2O_3], where there is a substantial excess of Na^+, the boron atoms are found to be predominantly in fourfold coordination, as evidenced by the very intense and narrow ^{11}B NMR resonance near −2 ppm in Fig. 5. With increasing [Al_2O_3], this peak remains the most intense spectral feature for most of the glasses, until the Al12.5 composition, where the intensity of the broad, asymmetric resonance centered around 10 ppm increases substantially. The latter feature is indicative of B^{III}, the relative population of which is sensitive to [Al_2O_3]. In the ^{11}B MAS NMR spectra, it reflects second-order quadrupolar line broadening due to lower symmetry around the B^{III} triangles than is found for the nearly symmetric B^{IV} units. The significant line shape differences for B^{III} triangles and B^{IV} tetrahedra are consistent with previous studies of boron coordination in simple modified borate glasses.[17,34] Such differences in line shape, especially when measured at sufficiently high magnetic fields to obtain separation of the two peaks, allow accurate quantification of the boron coordination and ultimately the fraction of B^{IV} (N_4). Here, N_4 was determined for all of the glasses by fitting the ^{11}B MAS NMR spectra to a series of three- and fourfold coordinated line shapes, the results of which are given in Table I. These data clearly show that N_4 is controlled by the excess modifier content of the glasses. Hence, for low [Al_2O_3], there is a significant amount of sodium available to convert boron from B^{III} to B^{IV}. As [Al_2O_3] increases and the effective modifier content decreases, N_4 decreases.

In the two glasses with the highest [Al_2O_3], where ^{27}Al NMR indicated all Na^+ is used for charge-balancing Al^{IV} groups, a very small fraction of B^{IV} is detected ($\leqslant$1%). These nonzero values of N_4 are determined from fitting the overlapping resonances in the ^{11}B MAS NMR spectra, which likely has some associated uncertainty. However, we have directly detected B^{IV} groups in the ^{11}B 3QMAS NMR spectra, where a weak but clearly present peak is found for B^{IV} groups in the Al17.5 glass (Fig. 6). Similar evidence for a small fraction of B^{IV} units in the Al20 glass was also obtained (data not shown), indicating that even for peraluminous compositions, a minor degree of network modification beyond Al^{IV} group stabilization occurs. This implies that, in the peraluminous regime, there is a competition for Na^+ between charge compensating Al^{IV} and B^{IV}. However, the formation of Al^{IV} is strongly favored over that of B^{IV}, since only minor concentrations of B^{IV} exist. In the peralkaline regime, Na^+ will first charge compensate all Al as Al^{IV}, and there is no competition for Na^+ between charge compensating Al^{IV} and B^{IV}, as confirmed by only Al^{IV} groups in the ^{27}Al NMR data.

In sodium borosilicates, the Dell and Bray model[21–23] is a frequently used empirical model to predict the composition dependence of N_4. It should be mentioned that [Al_2O_3] is not involved in the Dell and Bray model. In order to apply this model to the boroaluminosilicate glasses, we have taken [Na_2O] − [Al_2O_3] as the effective modifier concentration and have not considered the effect of aluminum speciation on the network connectivity. According to the Yun and Bray invocation of this model,[22] $N_4 = ([Na_2O] - [Al_2O_3])/[B_2O_3]$ when [Na_2O] − [Al_2O_3] < [B_2O_3] and $N_4 = 1$ when [Na_2O] − [Al_2O_3] > [B_2O_3] for our glasses ($SiO_2/B_2O_3 \geqslant 8$). The composition dependence of the N_4 values predicted from this model is plotted in Fig. 11. We note that these N_4 values are excessively high compared to the experimental values from the present study.

According to Du and Stebbins,[13] the experimental deviation of N_4 from the Dell and Bray model could be due to the energy

TABLE II. Isotropic chemical shift (δ_{CS}) and quadrupolar coupling parameters for ^{27}Al, ^{11}B and ^{23}Na using MAS and 3QMAS NMR data. The quadrupolar coupling product ($P_Q = C_Q(1 + \eta^2/3)^{1/2}$) was determined from 3QMAS NMR spectra of ^{27}Al and ^{23}Na as described in the text. Missing values for the Al0 glass are due to lack of ^{27}Al 3QMAS NMR data for this glass. Fitting of ^{11}B MAS NMR spectra (Ref. 45) provided further delineation between C_Q (quadrupolar coupling constant) and η (asymmetry parameter).

			^{11}B MAS NMR					
	^{27}Al 3QMAS NMR[a]		δ_{CS} (ppm)				^{23}Na 3QMAS NMR	
Glass ID	δ_{CS} (ppm)	P_Q (MHz)	[BO_3]	[BO_4]	C_Q (MHz)[b]	η[b]	δ_{CS} (ppm)	P_Q (MHz)
Al0			16.8	−1.1 −2.1	2.55	0.52	−3	3.5
Al1	61	4.2	16.9	−0.8 −1.9	2.55	0.53	−3	3.6
Al2.5	59	3.7	16.4	−1.1 −2.2	2.44	0.57	−5	2.4
Al5	59	4.1	16.7	−0.8 −1.9	2.52	0.57	−7	2.5
Al7.5	60	3.9	16.7	−0.5 −1.8	2.58	0.49	−9	2.3
Al10	60	3.9	16.4	−0.4 −2	2.62	0.48	−10	2.2
Al12.5	60	3.7	16.4	−0.4 −1.7	2.67	0.42	−12	2.1
Al15	61	4.0	16.2	−0.3 −1.8	2.67	0.38	−11	2.1
Al17.5	62	4.2	16 18.4	−0.5	2.63 2.75	0.22 0.22	−11	2.5
Al20	63	4.2	14 17	−0.5	2.59 2.67	0.25 0.31	−11	2.3

[a]NMR parameters were determined for only Al^{IV} groups using ^{27}Al 3QMAS NMR data.
[b]Quadrupolar coupling parameters for ^{11}B were only determined for the B^{III} sites, as C_Q and η for the tetrahedral B^{IV} units are small and therefore not included in the MAS NMR line shape simulations.

penalty from the mixing of B^{IV} and Al^{IV} groups, i.e., with the presence of negatively charged Al^{IV} groups, the formation of B^{IV} units is energetically unfavorable. For boroaluminosilicate glasses, Du and Stebbins[13] have developed a modified Dell–Bray model. This model groups Al and B as a single type of cation based on the consideration that the mixing behavior for Al^{IV} is similar to that of B^{IV} and the variation of N_4 is related to avoidance among B^{IV} and Al^{IV} species. Predicted values of N_4 for our glasses using this model are also plotted in Fig. 11. We find a certain degree of discrepancy between the Du–Stebbins model and our experimental results. The discrepancy could be attributed to the assumption that the mixing behavior for Al^{IV} is similar to that of B^{IV}. However, according to Du and Stebbins,[13] their model is not expected to accurately predict the N_4 of the glass system with the composition range of Al ≫ B. This is exactly the range where the discrepancy between the predicted and experimental N_4 values appears (Fig. 11). In spite of this apparent discrepancy, the Du–Stebbins model provides a good prediction of the N_4 variation with composition for the glasses studied in the present work.

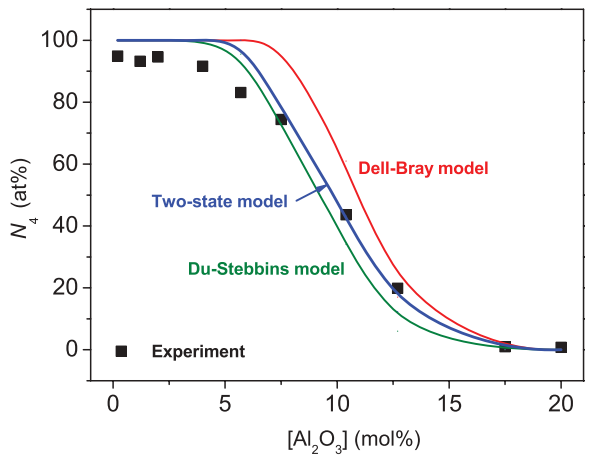

FIG. 11. (Color online) Comparison of the N_4 data obtained from NMR and three different models. The errors of the experimental N_4 values (±0.2%) are smaller than the size of the symbols.

C. Nonbridging oxygen formation

For both the Dell–Bray and Du–Stebbins models, N_4 values are overpredicted at low [Al_2O_3]. This suggests that, after charge compensating Al^{IV}, not all of the excess Na^+ ions are used in converting B^{III} to B^{IV}. Instead, some of the excess modifier is available for other types of network modification, in particular, formation of NBOs. It is well known that excess modifier can lead to formation of NBO on both boron and silicon.[35,36] In alkali borosilicates, this is apparent in the maximum value of N_4 for various compositions, at which point additional modifier is used to create NBO rather than

B^{IV}. Hence, the maximum value of N_4 is not 100%, similar to what we have observed for the low-Al_2O_3 glasses in this study.

The ^{11}B NMR spectra in Fig. 5 contain some evidence for NBO formation on B^{III}. However, due to the low fraction of B^{III} for glasses with alumina content smaller than that of Al10, such effects are difficult to identify. Vertical expansion of these spectra (not shown) indicates that the B^{III} line shape is changing with glass composition. For example, comparing the data for Al12.5 and Al20 reveals that the B^{III} line shape is noticeably different for different [Al_2O_3]. Simulations of the ^{11}B MAS NMR spectra, especially the resonances from B^{III}, confirm the presence of multiple environments, which differ in terms of the quadrupolar asymmetry parameter η. This parameter is shown in Table II for all B^{III} sites in these glasses. We find that it systematically changes with [Al_2O_3]. At high [Al_2O_3], where most of the sodium is used for stabilizing Al^{IV}, the value of η is relatively low (0.2 to 0.4). As the amount of excess modifier increases, the B^{III} asymmetry parameter also increases, reaching values as high as 0.57 for some of the low [Al_2O_3] compositions. Such values of η are typical of B^{III} having an asymmetric distribution of bridging and NBO, as would be the case for B^{III} units with one or two NBO.[23] Essentially, the ^{11}B MAS NMR line shape for B^{III} is changing from one comprised of all symmetric B^{III} units to one with at least some fraction of B^{III} with NBO. Thus, for glasses where the effective modifier concentration is nonzero and likely greater than ∼2 mol%, we detect formation of NBO on B^{III} atoms.

The ^{11}B 3QMAS NMR spectra appear to contain only a single B^{III} resonance, with the exception of the Al17.5 and Al20 glasses. This likely reflects a distribution of environments with average values of η higher than those in glasses having only symmetric B^{III} units, as discussed above for spectral simulation of the ^{11}B MAS NMR spectra. The inability to resolve distinct symmetric and asymmetric B^{III} line shapes in the 3QMAS NMR spectra (Fig. 6), makes accurate quantification of NBO on boron difficult, but nonetheless the presence of such units confirms the activity of excess effective modifier in peralkaline glasses. There are two glasses in which multiple B^{III} resonances were distinctly resolved in the ^{11}B 3QMAS NMR spectra: Al17.5 and Al20. These glasses are both peraluminous and already shown to contain almost exclusively B^{III}, and they appear to contain two symmetric (low η) B^{III} sites, reminiscent of ring and nonring B^{III} units in v-B_2O_3 and slightly modified borate glasses.[37,38] The isotropic chemical shifts for these resonances (Table II) are also consistent with symmetric B^{III} units in different superstructural or intermediate-range order environments.

In addition to changes in boron speciation, including both N_4 and NBO formation, the excess modifier in the peralkaline compositions can also impact the speciation of silicon. Nonbridging oxygen formation on Si, resulting in $Q^{n\neq4}$ [n is the number of bridging oxygens (BOs) per tetrahedral silicon], e.g., Q^3, Q^2 and other Si tetrahedra, is well known in alkali silicates and aluminosilicates.[39,40] One might expect similar behavior in the glasses studied here, in particular for those having the highest excess modifier concentrations. Therefore, ^{29}Si NMR data were collected to ascertain the Si speciation as a function of glass composition. ^{29}Si MAS NMR spectra show evolution of the signal with increasing [Al_2O_3] (Fig. 7). The nominally Al-free glass (Al0) contains two fairly well-resolved ^{29}Si resonances centered at approximately −96 and −108 ppm. In Al-free glasses, these peaks correspond well to Q^3 and Q^4 sites, respectively,[41,42] suggesting that the Al0 glass contains a moderate quantity of NBO on Si (e.g., Q^3 sites). The other glasses in this study contain nonnegligible concentrations of Al, and the presence of Al polyhedra as NNN to Si tetrahedra substantially complicates the interpretation and quantification of ^{29}Si MAS NMR spectra.[43,44] It is thus mostly due to increasing [Al_2O_3] that the peaks in the MAS NMR spectra in Fig. 7 move to less negative chemical shifts, since increasing Al NNN has this direct impact on Q^n chemical shifts. Notwithstanding this limitation, it does appear evident from the evolution in the ^{29}Si MAS NMR data that the spectra are simplified with increasing [Al_2O_3]. For glasses at the highest [Al_2O_3], the ^{29}Si line shape is much more symmetric and likely reflects fewer distinct Si species. This of course is expected based on the availability of modifier in these glasses, i.e., higher [Al_2O_3] reduces the amount of effective modifier available for NBO formation on Si, eventually eliminating any possibility for non-Q^4 groups.

D. Structural modeling

To further identify and estimate the NBO concentration on Si tetrahedra, static or wide-line ^{29}Si NMR measurements were conducted. As shown in Fig. 8, there is again a gradual change in the ^{29}Si spectra with glass composition, signifying some type of evolution in Si speciation. We first fit the Al1 spectrum using parameters which gave a reasonable fit and then froze those parameters (mainly line broadening and chemical shift anisotropy terms) in all subsequent fits. These wide-line ^{29}Si NMR spectra were fit with DMFit[45] and provided quantitative estimates for the relative amounts of Q^3 and Q^4 along the entire series of glasses (Table III). As with the ^{29}Si MAS NMR data, the Q^3 concentration drops steadily with increasing [Al_2O_3]. For [Al_2O_3] $\geqslant$ ∼12 mol%, the Q^3 fraction and thus the NBO on Si content goes to zero. For [Al_2O_3] above this level, the glasses apparently have insufficient modifier to stabilize Al^{IV} and B^{IV} groups, as well as formation of NBO on Si. In spite of the complications in accurately determining Q^3 populations in these glasses, due both to Al NNN complications and poor signal to noise, the ^{29}Si NMR data do show conclusively the presence and compositional dependence of NBO on Si tetrahedra, further demonstrating the many different modifier roles of Na in these glasses. The various NMR data indicate that after charge compensating Al^{IV}, not all of the excess Na_2O is used for converting B^{III} to B^{IV}. Instead some of the Na^+ ions are used to create NBO on both Si and B. There is a competition between converting B^{III} to B^{IV} and creating NBO. In order to quantify this effect, we next consider the two-state statistical mechanical model of boron speciation, which originally was developed for borosilicate glasses.[28]

According to the two-state model, the free energy associated with NBO formation on Si^{IV} takes an intermediate value compared to those of the B^{III} to B^{IV} conversion and NBO-on-B^{III} formation,[28,46–48] and this value appears close to the energy associated with B^{III} to B^{IV} conversion. We define

TABLE III. Q^n units calculated by the random model and measured by NMR for the boroaluminosilicate glasses as described and labeled in Table I. Q^{3}' is estimated for comparison to the NMR results by assuming $Q^2 = 2Q^3$ and ignoring the minor contributions from Q^1 in the random model.

	Random model						
Glass ID	Q^4 (%)	Q^3 (%)	Q^2 (%)	Q^1 (%)	Q^0 (%)	Q^{3}' (%)	NMR Q^3 (%)
Al0	77.28	20.57	2.05	0.09	0.00	24.68	33
Al1	79.41	18.85	1.68	0.07	0.00	22.20	24
Al2.5	81.33	17.25	1.37	0.05	0.00	19.99	18
Al5	86.11	13.12	0.75	0.02	0.00	14.62	12
Al7.5	90.72	8.95	0.33	0.01	0.00	9.61	5
Al10	95.89	4.04	0.06	0.00	0.00	4.17	2
Al12.5	97.90	2.08	0.02	0.00	0.00	2.12	0
Al15	100	0	0	0	0	0	0
Al17.5	100	0	0	0	0	0	0
Al20	100	0	0	0	0	0	0

ΔH as the enthalpy difference between NBO formation and B^{III} to B^{IV} conversion. Whether the modifiers are used for B^{III} to B^{IV} conversion or NBO-on-Si^{IV} formation is determined by the enthalpy difference between the two states (ΔH) and the number of available boron vs silicon sites (i.e., an entropic effect governed by the fictive temperature T_f and $[SiO_2]$ vs $[B_2O_3]$).

Since we have confirmed that all aluminum is in fourfold coordination when $[Na_2O] > [Al_2O_3]$, we can safely use $[Na_2O] - [Al_2O_3]$ to calculate the effective modifier concentration. When $[Na_2O] < [Al_2O_3]$, we state that $N_4 = 0$, which is close to the values determined from ^{11}B NMR. When $[Na_2O] > [Al_2O_3]$, N_4 can be calculated as

$$N_4 = \frac{[Na_2O] - [Al_2O_3]}{[B_2O_3] + [SiO_2]\exp[-\Delta H/kT_f]}, \quad (1)$$

where k is Boltzmann's constant. The fictive temperature T_f is taken as equal to the glass transition temperature (cooled at 10 K/s), i.e., $T_f = T_g$.[49] If ΔH is large, the modifiers are more likely to be used for charge-balancing B^{IV}, so N_4 will be large. With higher fictive temperatures and high SiO_2 concentrations, N_4 attains a lower value due to the effect of entropy. Using the experimentally determined values of $T_g = T_f$ listed in Table I, we obtain good agreement between the two-state model and the NMR results (Fig. 11) taking $\Delta H = 0.28$ eV as the sole fitting parameter. During the fit of ΔH, N_4 is constrained to be in the range of $0 \sim 1$. The uncertainty of ΔH is ± 0.01 eV. As shown in Fig. 11, the Dell–Bray model overpredicts N_4 and the Du–Stebbins model underpredicts N_4. The two-state model gives the best agreement with NMR data among these models. It should be noted that the two-state model has its limitations. First, the fictive temperature effect on N_4 applies only to silicate and boroaluminosilicate glasses, and this is seen from Eq. (1). For borate glasses, the effect of fictive temperature on N_4 also exists, but it is not considered in this model. Second, N_4 is predicted to increase monotonically with Na_2O content. Despite these limitations, the two-state model gives a relatively accurate description of the boron speciation for the glass compositions studied in the present work.

The random model, which is used to describe the distribution of Q^n units in silicate glasses, assumes a statistical distribution of Q^n units for discrete values of n between 0 and 4. Here, we apply this model to the boroaluminosilicate glasses. Following this model,[50–52] we first calculate the probability (p) that a randomly chosen Si-O bond includes a NBO. It is equal to the ratio between the number of NBOs and the total number of bonds [NBO] + [BO], where BO is a bridging oxygen. For silicate glasses, $p = \mathrm{NBO}/(Z[Si^{IV}])$, where Z is the coordination number of the network former. For our aluminoborosilicate glasses, $p = \mathrm{NBO}/(4[Si^{IV}] + 3[B^{III}])$, since NBOs exist both on Si^{IV} and B^{III}, i.e., the existence of B^{III} lowers the probability for a NBO to be associated with Si. Since addition of sodium to boroaluminosilicate glasses results in the formation of Al^{IV}, B^{IV}, and/or NBO, the concentration of NBOs can be calculated as $2([Na_2O] - [Al^{IV}] - [B^{IV}])$. By using

$$Q^n = \frac{4!}{n!(4-n)!}(1-p)^n p^{4-n}, \quad (2)$$

the Q^n values are calculated and listed in Table III. In order to compare the calculated values of Q^n to the Q^3 and Q^4 values obtained from NMR, one Q^2 unit was counted as two Q^3 units and Q^1 and Q^0 units were ignored, since their concentrations are predicted to be less than 1%. Figure 12 shows that Q^3 calculated by the random model agrees well with that measured by NMR, viz., Q^3 decreases as $[Al_2O_3]$ increases. The discrepancy at Al0, which is the data point having the most accuracy, indicates that the random model does not work well for all glasses in this series. Without Al_2O_3 in the glass, all of the Na^+ is being consumed by B^{IV} and NBO, the latter of which is essentially all on Si as determined by both ^{11}B and ^{29}Si NMR. This situation, which is perhaps unique to this particular glass composition, is reflected in the higher Q^3 population of Fig. 12.

E. Structural role of sodium

The local Na^+ environment is significantly impacted by $[Al_2O_3]$. The broad ^{23}Na MAS line shapes at low $[Al_2O_3]$ suggest multiple or at least a large distribution of sodium environments (Fig. 9). They are likely from Na^+ as a charge-balancing cation for B^{IV}, NBO on boron and/or silicon, as well as a small fraction of Al^{IV}. The ^{23}Na MAS line shapes

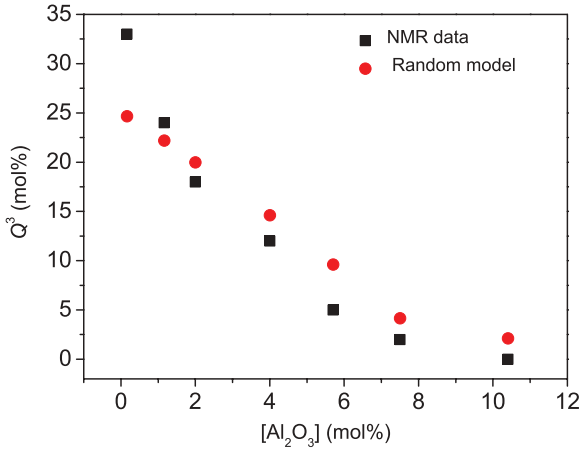

FIG. 12. (Color online) Comparison of Q^3 data calculated by the random model and measured by NMR of the boroaluminosilicate glasses as described and labeled in Table I. The error range of the NMR data is $\pm 5\%$.

narrow considerably at higher $[Al_2O_3]$, suggesting a more uniform environment (and role) of Na^+ ions, i.e., they are mostly used to charge balance Al^{IV} at the higher $[Al_2O_3]$. The ^{23}Na 3QMAS NMR spectra confirm changes in the ^{23}Na resonance with increasing $[Al_2O_3]$, as well as the fact that only one distinct sodium environment is resolved for all of the glasses. Both δ_{CS} and P_Q of ^{23}Na vary for these glasses as a function of composition, with an initial decrease in δ_{CS} with increasing $[Al_2O_3]$, until at $[Al_2O_3] \sim 10$ mol%, where the ^{23}Na chemical shift levels at a value of -10 to -12 ppm. The initial decrease in chemical shift correlates very well with the increasing amount of Al^{IV} groups that require Na cations for charge compensation. These Al^{IV} groups, as well as B^{IV} groups, are negatively charged polyhedra which do not possess NBO atoms.

It has been reported that, in glasses where Na is the only non-network forming cation, δ_{CS} for ^{23}Na increases systematically with increasing $[Na_2O]$, in part because of increasing fraction of NBO in the average Na coordination shells and the accompanying shortening of mean Na-O distances.[14,26,53] In our glass systems, δ_{CS} decreases with an increase in $[Al_2O_3]$, indicating that the NBO content is decreasing as well. This agrees well with our direct determination of NBO content, where both ^{11}B and ^{29}Si NMR spectra show a decrease in the NBO content with increasing $[Al_2O_3]$. As $[Al_2O_3]$ increases, more Na^+ ions are required for stabilizing Al^{IV} groups until this is essentially the only environment for Na, i.e., an environment without any NBO in the local coordination environment. Similarly, we find a marked decrease in P_Q with increasing $[Al_2O_3]$, consistent with a more uniform coordination environment as well as an increase in the average coordination number of Na.[14,26,53] Both observations reflect changes from multiple Na sites (i.e., structural roles) to a relatively uniform distribution of Na^+ in Al^{IV} charge-balancing positions, and the increase in Na coordination number simply reflects fewer NBO in its coordination sphere as these species diminish with increasing $[Al_2O_3]$. Finally, it should be mentioned that the change in the Na environment with composition is a continuous variation in the types and numbers of different kinds of oxygen, e.g., NBO vs various BO (connected to Si or B or Al) in the average Na coordination shell. This aspect will be closely studied in our future work.

V. SUMMARY

We have studied the structure of ten Na_2O-B_2O_3-Al_2O_3-SiO_2 glasses with varying $[Al_2O_3]/[SiO_2]$ ratio to access different regimes of sodium behavior. The network speciation and modifier cation environments have been characterized as a function of composition using multinuclear NMR spectroscopy. Based on these NMR results, the different roles of sodium with respect to the network-forming cations (Si, B, and Al) have been clarified and quantified. We confirm that when $[Na_2O] < [Al_2O_3]$, almost all sodium is used to charge compensate Al^{IV}; however, there are also Al^V species which act as charge compensators due to insufficient sodium. When $[Na_2O] > [Al_2O_3]$, sodium first charge compensates Al^{IV}, i.e., all aluminum is fourfold coordinated, and there is no compositional dependence of the aluminum speciation. After charge compensating Al^{IV}, not all of the excess Na^+ ions are used for converting B^{III} to B^{IV}, since some are used to create NBOs on both Si and B. This indicates a competition in the boroaluminosilicate glasses between B^{III} to B^{IV} conversion and NBO formation. Consequently, we have found that the Dell–Bray and Du–Stebbins models do not fully predict values of N_4 determined experimentally, since both models do not account for such competition. To account for this competition, we have extended our two-state statistical mechanical model of boron speciation developed for borosilicate glasses to boroaluminosilicate glasses. By doing so, we have obtained better agreement between the predicted and measured values of N_4. Furthermore, the composition dependence of Q^3 has been described by using a random model that agrees well with the experimental values obtained from ^{29}Si wide-line NMR spectroscopy.

ACKNOWLEDGMENTS

The authors would like to thank Adam Ellison (Corning Incorporated) for valuable discussion on glass composition and characterization approaches.

*Corresponding author: youngmanre@corning.com

[1] S. K. Lee, G. D. Cody, Y. W. Fei, and B. O. Mysen, Chem. Geol. **229**, 162 (2006).
[2] G. Yang, B. Bureau, T. Rouxel, Y. Gueguen, O. Gulbiten, C. Roiland, E. Soignard, J. L. Yarger, J. Troles, J. C. Sangleboeuf, and P. Lucas, Phys. Rev. B **82**, 195206 (2010).
[3] G. N. Greaves, J. Non-Cryst. Solids **71**, 203 (1985).
[4] M. Hanaya and R. K. Harris, J. Phys. Chem. A **101**, 6903 (1997).
[5] J. F. Stebbins and Z. Xu, Nature **390**, 60 (1997).
[6] M. Bauchy, M. Micoulaut, M. Celino, S. Le Roux, M. Boero, and C. Massobrio, Phys. Rev. B **84**, 054201 (2011).

[7]Q. J. Zheng, M. Potuzak, J. C. Mauro, M. M. Smedskjaer, R. E. Youngman, and Y. Z. Yue, J. Non-Cryst. Solids **358**, 993 (2012).
[8]F. Angeli, O. Villain, S. Schuller, T. Charpentier, D. de Ligny, L. Bressel, and L. Wondraczek, Phys. Rev. B **85**, 054110 (2012).
[9]S. Sen, T. Topping, P. Yu, and R. E. Youngman, Phys. Rev. B **75**, 094203 (2007).
[10]N. Ollier, T. Charpentier, B. Boizot, and G. Petite, J. Phys.: Condens. Matter **16**, 7625 (2004).
[11]F. Angeli, T. Charpentier, S. Gin, and J. C. Petit, Chem. Phys. Lett. **341**, 23 (2001).
[12]J. M. Egan and K. T. Mueller, J. Phys. Chem. B **104**, 9580 (2000).
[13]L. S. Du and J. F. Stebbins, J. Non-Cryst. Solids **351**, 3508 (2005).
[14]J. S. Wu and J. F. Stebbins, J. Non-Cryst. Solids **355**, 556 (2009).
[15]J. S. Wu and J. F. Stebbins, J. Non-Cryst. Solids **356**, 2097 (2010).
[16]L. S. Du and J. F. Stebbins, J. Non-Cryst. Solids **315**, 239 (2003).
[17]R. E. Youngman and J. W. Zwanziger, J. Phys. Chem. **100**, 16720 (1996).
[18]F. Angeli, T. Charpentier, D. D. Ligny, and C. Cailleteau, J. Am. Ceram. Soc. **93**, 2693 (2010).
[19]M. M. Smedskjaer, J. C. Mauro, S. Sen, and Y. Z. Yue, Chem. Mater. **22**, 5358 (2010).
[20]A. Vegiri, C. P. E. Varsamis, and E. I. Kamitsos, Phys. Rev. B **80**, 184202 (2009).
[21]W. J. Dell, P. J. Bray, and S. Z. Xiao, J. Non-Cryst. Solids **58**, 1 (1983).
[22]Y. H. Yun and P. J. Bray, J. Non-Cryst. Solids **27**, 363 (1978).
[23]J. H. Zhong and P. J. Bray, J. Non-Cryst. Solids **111**, 67 (1989).
[24]H. Yamashita, H. Yoshino, K. Nagata, H. Inoue, T. Nakajin, and T. Maekawa, J. Non-Cryst. Solids **270**, 48 (2000).
[25]H. Yamashita, K. Inoue, T. Nakajin, H. Inoue, and T. Maekawa, J. Non-Cryst. Solids **331**, 128 (2003).
[26]J. F. Stebbins, Solid State Ionics **112**, 137 (1998).
[27]S. K. Lee and J. F. Stebbins, Geochim. Cosmochim. Acta **67**, 1699 (2003).
[28]M. M. Smedskjaer, J. C. Mauro, R. E. Youngman, C. L. Hogue, M. Potuzak, and Y. Z. Yue, J. Phys. Chem. B **115**, 12930 (2011).
[29]J. C. Mauro, Y. Z. Yue, A. J. Ellison, P. K. Gupta, and D. C. Allan, Proc. Natl. Acad. Sci. USA **106**, 19780 (2009).
[30]J. P. Amoureux, C. Fernandez, and S. Steuernagel, J. Magn. Reson. A **123**, 116 (1996).
[31]S. H. Risbud, R. J. Kirkpatrick, A. P. Taglialavore, and B. Montez, J. Am. Ceram. Soc. **70**, C-10 (1987).
[32]S. Sen and R. E. Youngman, J. Phys. Chem. B **108**, 7557 (2004).
[33]D. R. Neuville, L. Cormier, and D. Massiot, Geochim. et Cosmochim. Acta **68**, 5071 (2004).
[34]R. E. Youngman and J. W. Zwanziger, J. Am. Chem. Soc. **117**, 1397 (1995).
[35]D. Manara, A. Grandjean, and D. R. Neuville, Am. Mineral. **94**, 777 (2009).
[36]A. C. Wright, Phys. Chem. Glasses: Eur. J. Glass Sci. Technol. B **51**, 1 (2010).
[37]R. E. Youngman and J. W. Zwanziger, J. Non-Cryst. Solids **168**, 293 (1994).
[38]S. Sen, Z. Xu, and J. F. Stebbins, J. Non-Cryst. Solids **226**, 29 (1998).
[39]E. Schneider, J. F. Stebbins, and A. Pines, J. Non-Cryst. Solids **89**, 371 (1987).
[40]J. F. Stebbins, J. Non-Cryst. Solids **106**, 359 (1988).
[41]E. Lippmaa, M. Mägi, A. Samoson, G. Engelhardt, and A. R. Grimmer, J. Am. Chem. Soc. **102**, 4889 (1980).
[42]M. Mägi, E. Lippmaa, G. Engelhardt, and A. R. Grimmer, J. Phys. Chem. **88**, 1518 (1984).
[43]S. K. Lee and J. F. Stebbins, J. Phys. Chem. B **104**, 4091 (2000).
[44]S. K. Lee and J. F. Stebbins, J. Non-Cryst. Solids **270**, 260 (2000).
[45]D. Massiot, F. Fayon, M. Capron, I. King, S. Le Calvé, B. Alonso, J. Durand, B. Bujoli, Z. Gan, and G. Hoatson, Magn. Reson. Chem. **40**, 70 (2002).
[46]R. J. Araujo, J. Non-Cryst. Solids **42**, 109 (1980).
[47]R. J. Araujo, J. Non-Cryst. Solids **58**, 201 (1983).
[48]R. J. Araujo, J. Non-Cryst. Solids **81**, 251 (1986).
[49]Y. Z. Yue, J. Non-Cryst. Solids **354**, 1112 (2008).
[50]M. Moesgaard, R. Keding, J. Skibsted, and Y. Z. Yue, Chem. Mater. **22**, 4471 (2010).
[51]J. F. Stebbins, J. Non-Cryst. Solids **106**, 359 (1988).
[52]I. Avramov, C. Rüssel, and R. Keding, J. Non-Cryst. Solids **324**, 29 (2003).
[53]L. M. Peng and J. F. Stebbins, J. Non-Cryst. Solids **353**, 4732 (2007).